The Astrophysical Journal, 756:150 (6pp), 2012 September 10 doi:10.1088/0004-637X/756/2/150

HUBBLE SPACE TELESCOPE NARROWBAND SEARCH FOR EXTENDED Lyα EMISSION AROUND TWO $z > 6$ QUASARS

Roberto Decarli[1], Fabian Walter[1], Yujin Yang[1], Chris L. Carilli[2,3], Xiahoui Fan[4], Joseph F. Hennawi[1], Jaron Kurk[5], Dominik Riechers[6], Hans-Walter Rix[1], Michael A. Strauss[7], and Bram P. Venemans[1]
[1] Max-Planck Institut für Astronomie, Königstuhl 17, D-69117 Heidelberg, Germany; decarli@mpia.de
[2] NRAO, Pete V. Domenici Array Science Center, P.O. Box O, Socorro, NM 87801, USA
[3] Astrophysics Group, Cavendish Laboratory, JJ Thomson Avenue, Cambridge CB3 0HE, UK
[4] Steward Observatory, University of Arizona, 933 North Cherry Avenue, Tucson, AZ 85721, USA
[5] Max-Planck-Institut für Extraterrestrische Physik, Gießenbachstraße 1, D-85748 Garching, Germany
[6] Astronomy Department, Caltech, 1200 East California boulevard, Pasadena, CA 91125, USA
[7] Department of Astrophysical Sciences, Princeton University, Peyton Hall, Ivy Lane, Princeton, NJ 08544, USA
Received 2012 April 18; accepted 2012 July 5; published 2012 August 23

ABSTRACT

We search for extended Lyα emission around two $z > 6$ quasars, SDSS J1030+0524 ($z = 6.309$) and SDSS J1148+5251 ($z = 6.419$) using Wide Field Camera 3 narrowband filters on board the *Hubble Space Telescope*. For each quasar, we collected two deep, narrowband images, one sampling the Lyα line+continuum at the quasar redshifts and one of the continuum emission redward of the line. After carefully modeling the point-spread function, we find no evidence for extended Lyα emission. These observations set 2σ limits of L(Lyα, extended) $<3.2 \times 10^{44}$ erg s^{-1} for J1030+0524 and L(Lyα, extended) $<2.5 \times 10^{44}$ erg s^{-1} for J1148+5251. Given the star formation rates typically inferred from (rest-frame) far-infrared measurements of $z \sim 6$ quasars, these limits are well below the intrinsic bright Lyα emission expected from the recombination of gas photoionized by the quasars or by the star formation in the host galaxies, and point toward significant Lyα suppression or dust attenuation. However, small extinction values have been observed along the line of sight to the nuclei, thus reddening has to be coupled with other mechanisms for Lyα suppression (e.g., resonance scattering). No Lyα emitting companions are found, down to a 5σ sensitivity of $\sim 1 \times 10^{-17}$ erg s^{-1} cm^{-2} arcsec^{-2} (surface brightness) and $\sim 5 \times 10^{-17}$ erg s^{-1} cm^{-2} (assuming point sources).

Key words: galaxies: formation – galaxies: halos – quasars: general – quasars: individual (J1030+0524, J1148+5251)

Online-only material: color figures

1. INTRODUCTION

The host galaxies of very high z quasars ($z > 6$), harboring $>10^9 M_\odot$ black holes, are thought to reside in the highest density peaks in the universe (e.g., Volonteri & Rees 2006). Abundant cold gas reservoirs are necessary to feed the black hole growth in such a short time (the universe at $z = 6$ is less than 1 Gyr old). Such gas reservoirs would also likely be sites of extensive star formation. Studying host galaxies of quasars at $z \sim 6$ is therefore one way to study the buildup of the first massive galaxies.

Indeed, a large fraction (30%–50%) of the $z > 5$ quasars observed at (sub-)millimeter wavelengths have been detected, revealing far-infrared (FIR) luminosities $5 \times 10^{12} - 2 \times 10^{13}\ L_\odot$ (Priddey et al. 2003; Bertoldi et al. 2003; Wang et al. 2008b, 2011; Leipski et al. 2010). The spectral energy distributions (SEDs) of these objects suggest that star formation (rather than black hole accretion) is powering dust heating (Beelen et al. 2006; Leipski et al. 2010; Wang et al. 2011). The associated star formation rates (SFRs) easily exceed several hundred $M_\odot$ yr^{-1}. Such high SFRs are in agreement with the detection of bright [C II]$_{158\,\mu\mathrm{m}}$ emission that is extended on kpc scales (e.g., Maiolino et al. 2005; Walter et al. 2009). Similarly, direct evidence for significant molecular gas reservoirs, exceeding $10^{10}\ M_\odot$, in $z \sim 6$ quasar host galaxies has now been firmly established through observations of the redshifted CO emission (Bertoldi et al. 2003; Walter et al. 2003, 2004; Carilli et al. 2007; Wang et al. 2007, 2011; Riechers et al. 2009).

Despite these increasing observational constraints, several questions remain unanswered: How do quasar host galaxies accrete their gas? Is the gas dynamically cold, and accreting through filaments (see, e.g., Haiman & Rees 2001; Dekel et al. 2009; Dubois et al. 2012; Di Matteo et al. 2012)? Are host galaxies severely obscured? What is the escape fraction of UV and Lyα photons produced in these supposedly huge star formation events (Dayal et al. 2009)?

Key information to address these questions may come from the detection of extended UV and Lyα emission around high-z quasars, in particular the luminosity, physical extent, and morphology of their host galaxies and halos. Extended Lyα emission around radio galaxies and low-z quasars has been reported in the literature (e.g., Reuland et al. 2003; Weidinger et al. 2005; Francis & McDonnell 2006; Christensen et al. 2006; Barrio et al. 2008; Smith et al. 2009); however, so far deep observations have only been performed for one $z \sim 6$ quasar, J2329−0301 (Goto et al. 2009, 2012; Willott et al. 2011), using ground-based imaging and spectroscopic observations.

The present study aims to detect extended Lyα emission around two $z > 6$ quasars (for which suitable narrowband filters exist) SDSS J103027.10+052455.0 (Fan et al. 2001, $z = 6.309$; hereafter, J1030+0524) and SDSS J114816.64+525150.3 (Fan et al. 2003, $z = 6.419$; hereafter J1148+5251). The unique angular resolution offered by the *Hubble Space Telescope* (*HST*) allows us to disentangle the unresolved quasar light from any extended emission. We use the new narrowband imaging capabilities offered by the Wide Field Camera 3 (WFC3) in order

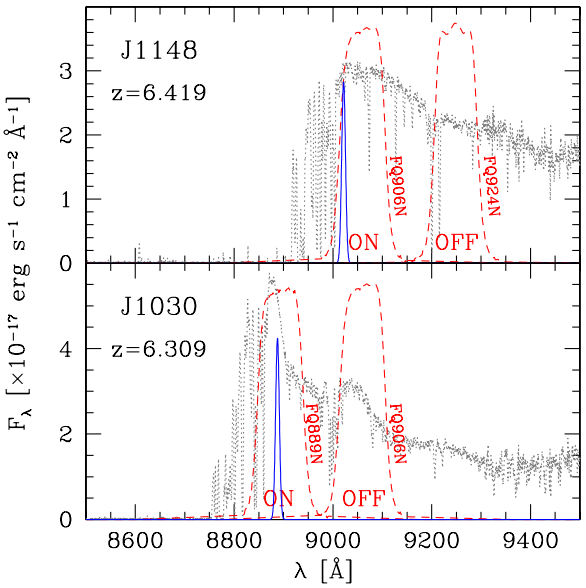

Figure 1. Spectra of J1030+0524 and J1148+5251 (gray, dotted lines) compared with the throughput curves of the filters used in our analysis (red, dashed lines) and with the expected profile of a 300 km s^{-1} broad Lyα line arising from the host galaxy (blue, solid lines). The redshift of the host galaxy is accurately defined by CO and [C II] observations for J1148+5251, and by the quasar Mg II line for J1030+0524. Spectra of the two quasars are taken from Pentericci et al. (2002) and Fan et al. (2003).

(A color version of this figure is available in the online journal.)

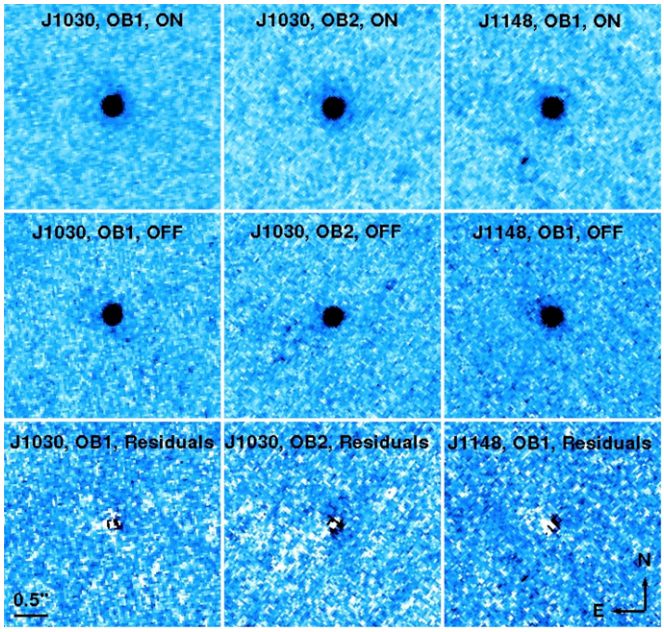

Figure 2. Line+continuum (ON, top row), continuum (OFF, middle row), and residual images of J1030+0524 and J1148+5251 in the three OBs used in our analysis. Residual images are obtained as the difference between ON and OFF frames, after scaling the latter in order to match the flux of the former in the central 5 × 5 pixels. The stretch of the color scale is linear. The scale and orientation of the images are the same in all the panels, as labeled in lower left, lower right, respectively. For a comparison, the starburst traced by [C II] emission observed by Walter et al. (2009) in J1148+5251 has a physical extension of ∼0.″3, while the molecular gas is distributed on scales of ∼0.″5 (Walter et al. 2004). No significant pure-line emission is detected around the quasar PSFs.

(A color version of this figure is available in the online journal.)

to sample both the pure continuum ("OFF" images) redward of Lyα and the Lyα + continuum ("ON" images). Through accurate modeling of the point-spread function (PSF) and its uncertainties, we will be able to constrain the presence of extended emission around the target quasars.

Throughout the paper we will assume a standard cosmology model with $H_0 = 70$ km s^{-1} Mpc^{-1}, $\Omega_m = 0.3$, and $\Omega_\Lambda = 0.7$.

2. WFC3 OBSERVATIONS

We use the "quad-filters," i.e., a set of four different narrow-band filters, each covering simultaneously about one-sixth of the WFC3/UVIS field of view (∼1 arcmin^2). For J1030+0524 (J1148+5251), we used the FQ889N (FQ906N) filter for the ON images and FQ906N (FQ924N) for the OFF images. Figure 1 illustrates the throughput curves of the adopted filters, the spectra of the quasars, and the redshift of the predicted Lyα emission from their host galaxies. The redshift is accurately defined by the CO and [C II] redshift of the source in the case of J1148+5251 and by the Mg II line for J1030+0524.

Observations were carried out during *HST* Cycle 17 (proposal ID: 11640). J1030+0524 was observed in two complete Observing Blocks (OBs; executed on 2010 January 28 and 2011 January 15) in both the ON and OFF setups (total integration time per OB: 5660 s in the ON setup, 5633 s in the OFF setup). During each OB, the ON and OFF observations were performed subsequently in an ON–OFF–OFF–ON sequence. J1148+5251 was observed once (2011 March 6) in the ON and OFF setups (total integration time: 6183 s for the ON setup, 6167 s for the OFF setup).

Our analysis is based on data products delivered by the *HST* pipeline. Photometry is defined following the WFC3 handbook.[8] Theoretical zero points in the AB system are computed based on the PHOTFLAM and PHOTPLAM keywords and further corrected to account for the deviations from on-sky to theoretical zero points.

Figure 2 shows the pipeline-reduced images of J1030+0524 and J1148+5251 in the three OBs used in this study. We do not stack the two OBs available for J1030+0524, in order to preserve the PSF properties in the two observations (collected on different dates), and to have a better control of the noise properties of the background.

The measured aperture magnitudes of the two quasars in all the OBs are consistent within 0.2 mag with the expected fluxes as derived from the spectroscopy (see Figure 1). This small difference is likely due to absolute flux calibration uncertainties, slit flux losses in the spectra, and intrinsic quasar variability.

3. PSF MODELS

In order to put constraints on extended Lyα emission in our targets, we need to model the dominant emission due to the central (unresolved) quasar. A common practice in quasar host galaxy studies is to model the quasar emission based on the images of foreground stars in the field (see, e.g., Kotilainen et al. 2009). This approach is sensitive to spatial variations of the PSF across the field. In order to evaluate these variations, we compare the radial profile of three stars in the field of J1030+0524 (OB2, ON; the field of J1148+5251 does not contain suitable stars and therefore cannot be used for this experiment). Figure 3 (left) shows the surface brightness profiles of these sources after the subtraction of a common Tiny Tim PSF model centered at the quasar position. The PSF quality degrades (i.e., PSF wings

[8] http://www.stsci.edu/hst/wfc3/phot_zp_lbn

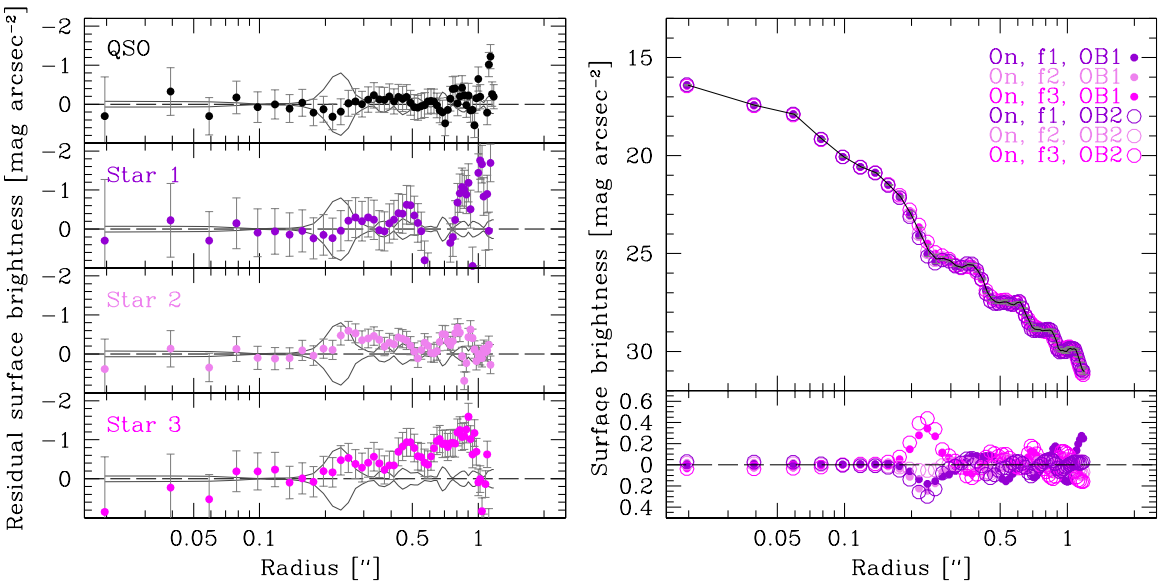

Figure 3. PSF variations due to field degradation (left panel) and *HST* breathing ("focus;" right panel) for J1030+0524 in the FQ889N filter. Left: difference between the PSF-subtracted light profiles of J1030+0524 and other unresolved sources in its field. Significant variations are observed. The PSF model is chosen to reproduce a point source at the quasar position, while the field stars are 16″, 44″, and 52″ from it, respectively. The solid lines show PSF model uncertainties (see Section 3 for details). Right: radial profiles of the Tiny Tim PSF models corresponding to the average (f1), the maximum (f2), and the minimum (f3) focus values. In the bottom panel, the residuals after the subtraction of the average PSF are shown.

(A color version of this figure is available in the online journal.)

are more prominent) as the distance from the quasar position increases. Thus the PSF of field stars cannot be used as a model for the quasar PSF.

Alternatively, one can use the OFF frames (including only the continuum emission) to model the quasar image in the ON images. The major advantage here is that the frames are always centered on the target (i.e., field variations of the PSF are minimized) and observations are carried out with the same focus conditions. However, this approach relies on the hypothesis that the quasar host galaxy does not show any extended emission in the continuum, which is an assumption we first need to test.

We therefore use *HST* PSF models as simulated using Tiny Tim. According to the WFC3 handbook, the PSF FWHM shows ∼0.3% variations as a function of the *HST* "breathing" (i.e., focus variations due to various causes, including thermal expansion of the satellite) at 800 nm, decreasing with increasing wavelength. According to focus variation models,[9] the focus changed significantly during the execution of the OBs. Nevertheless, variations of the PSF at these wavelengths are limited: Figure 3 (right) compares the radial light profile of the model PSF at the average, highest, and lowest values of the focus during the execution of the various OBs. The most important variations appear at aperture radii between 0.″2 and 0.″3. From these models, we adopt the PSF models that best match the observed quasar profile at these radii.

PSF uncertainties shown in Figure 3 are defined as the quadrature sum of the PSF variations due to focus fluctuations and formal uncertainties in the PSF profile due to pixelization, Poissonian errors, and background rms.

4. RESULTS

In this section we describe how we use these data to search for Lyα emission arising from the host galaxies (Section 4.1), from any filamentary structure around the quasars (Section 4.2), and from possible companion sources (Section 4.3). We then present the results for our two sources.

4.1. Extended Lyα Emission in the Host Galaxies

In order to investigate the presence of any extended emission arising from the host galaxies of our targets, we compare the observed ON and OFF light profiles of the observed quasars with those of the PSF models (Figure 4). The PSF model is normalized to match the observed total flux of the quasar. Using GALFIT (ver. 3.0.2; Peng et al. 2002, 2010), we simulate the light profile of a host galaxy of total magnitudes 19, 20, 21, and 22 mag (AB system). We assumed a Sérsic profile with ellipticity = 0.5, R_e = 1″, 0.″5, and 0.″14 (1″ ≈ 5.5 kpc at the redshift of our targets) and n_s = 2. The sampled range of effective radii is defined to reproduce the size of the Lyα extended emission reported by Willott et al. (2011) in J2329−0301 at z = 6.417 (diameter of ∼15 kpc) and more compact CO and [C II] emission in the host galaxy of J1148+5251, as reported by Walter et al. (2004) and Riechers et al. (2009; CO: 2.5 kpc) and Walter et al. (2009; [C II]: 1.5 kpc). We find that our results are practically independent of the ellipticity and the effective radius of the host galaxy model for 0.″14 < R_e < 1″.

4.2. Signatures of Gas Accretion

According to the models by Haiman & Rees (2001), the Lyα emission arising from gas surrounding quasar host galaxies at high-z can be as bright as 10^{-16} erg s^{-1} cm^{-2} arcsec^{-2}. More recently, Goerdt et al. (2010) showed that cold gas accreting can give rise to significant (up to few times 10^{-17} erg s^{-1} cm^{-2} arcsec^{-2} for relatively massive galaxies at z = 2.5) Lyα emission on 10–100 kpc scales. Such streams are potentially able to survive quasar feedback at very high z (Di Matteo et al. 2012).

In order to identify any pure-line extended emission around the quasars, we create "residual" images by subtracting properly

[9] http://www.stsci.edu/hst/observatory/focus/FocusModel/#5

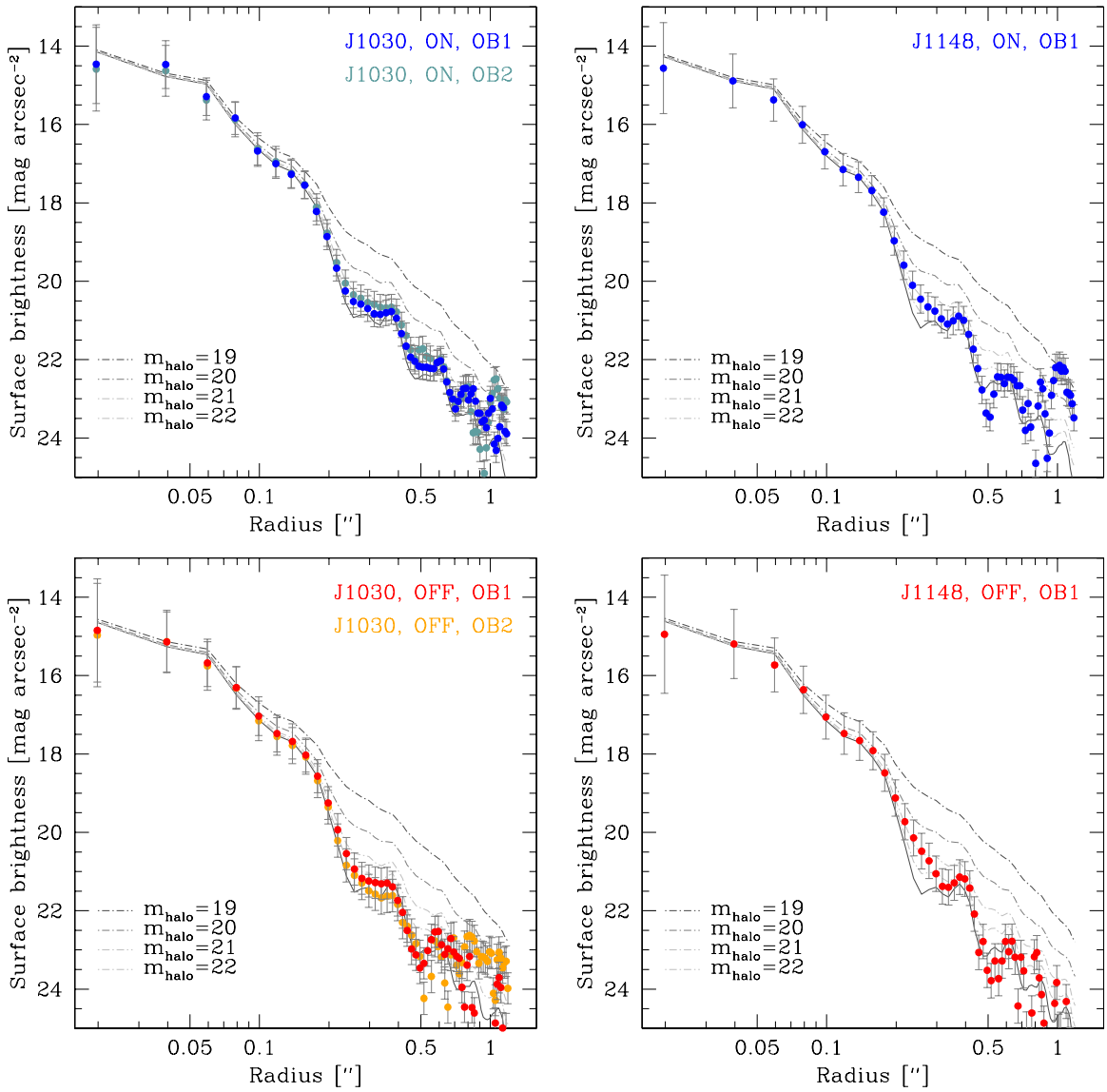

Figure 4. ON and OFF light profiles of J1030+0524 (left panels) and J1148+5251 (right panels). The expected profile for a point source plus a host galaxy with a Sérsic profile with $R_e = 1''$, $n_s = 2$, ellipticity = 0.5, and magnitude (of the extended component only) of 19, 20, 21, and 22 mag are plotted with dotted lines from dark to light gray. Error bars are computed as a combination of Poissonian errors, pixelizations, and background rms. No obvious extended emission is observed in any of the panels: the light profiles of the two targets are fully consistent with the unresolved emission from the quasars. Hosts of total magnitude = 21 would have been detected in our observations with $>2\sigma$ significance.

(A color version of this figure is available in the online journal.)

scaled OFF images from the line+continuum images ("ON"). The scaling is set to match the total flux observed in the central 5 × 5 pixels (≈0.″2 × 0.″2, roughly corresponding to the core of the PSF). The resulting "residual" images therefore are quasar-subtracted and allow us to investigate the presence of any extended, pure-line emission around the quasars (Figure 2, bottom panels).

4.3. Lyα Emitting Companions

Finally, we compare the sources detected in the ON images with those in the OFF images, in order to look for Lyα emitters in the field of our quasars. The FQ889N and FQ906N filters are sensitive to Lyα emission arising from objects in the redshift ranges $6.279 < z < 6.355$ and $6.415 < z < 6.492$, respectively, each corresponding to a comoving volume of ≈0.18 Mpc^3 (in the 1 arcmin^2 field of view). The 5σ detection limit for point sources in these two filters is 23.43 mag and 23.37 mag (1.9×10^{-16} erg s^{-1} cm^{-2} and 1.5×10^{-16} erg s^{-1} cm^{-2}), respectively. The observed number density of Lyα emitters exceeding this flux limit in a blank field at $z \sim 6.2$ is $\sim 10^{-3}$ Lyα emitter per arcmin^2 (e.g., Ouchi et al. 2010). This implies that no Lyα emitter is expected in this volume, for any reasonable overdensity, given our sensitivity.

4.4. Results for J1030+0524

The light profiles of J1030+0524 (Figure 4) do not show any extended component. The small light excesses in the OFF observations (of both OBs) at radii $\gtrsim 0.''5$ are due to cosmic-ray residuals which are observed in different positions in the two OBs (see Figure 2). We can set an upper limit to the magnitude of the extended component by comparing the observed profile with the ones simulated using GALFIT. We

focus on the 0.″2–0.″8 scale, i.e., where the deviations from a PSF are expected to be significant but the signal is still high and the PSF models are still reliable. Given the uncertainties in the observed light profiles and in the PSF model, a host of ≈21 mag for both the line and the continuum, is ruled out at 2σ. Assuming a Gaussian model for the Lyα line emission, with FWHM = 300 km s^{-1} and centered at the redshift of the quasar ($z = 6.309$, see Figure 1), we convert the limit set by the ON images into an Lyα flux limit taking into account the actual throughput curve of the filter and the redshift of the quasar host. We find F(Lyα,host) $<7.1 \times 10^{-16}$ erg s^{-1} cm^{-2}, i.e., L(Lyα,host) $<8.3 \times 10^{10}\,L_{\odot}$ or $<3.2 \times 10^{44}$ erg s^{-1}. For the continuum, assuming an SED with constant F_{ν} for the k-correction, we obtain a limit on the UV rest-frame luminosity of the host of $M_{1450} > -25.8$ mag.

A visual inspection of the "Residual" images reveals no significant filamentary structure within few arcsec of the source. The comparison between the images of the two OBs allows us to discard all the low-significance blobs within 5″ from the quasar as cosmic-ray residuals. We estimate a 5σ surface brightness sensitivity of $\sim 1 \times 10^{-17}$ erg s^{-1} cm^{-2} arcsec^{-2} (using a 1 arcsec^2 aperture). As expected, no Lyα emitter is found in the 1 arcmin^2 field around the quasar, down to a point-source sensitivity of 2.5×10^{43} erg s^{-1} (5-σ).

4.5. Results for J1148+5251

The light profile of J1148+5251 also does not show any extended component. In this case a small excess is seen at ∼1″ in the ON observation. This is most likely due to an observational artifact (see below). Following the same approach as adopted for J1030+0524, we can exclude a host galaxy brighter than ≈21 mag in the ON image (the light profile being perfectly consistent with a point source), and ≈21 mag for the continuum. These limits yield an Lyα flux from the host of $<5.4 \times 10^{-16}$ erg s^{-1} cm^{-2}, i.e., L(Lyα,host) $<6.6 \times 10^{10}\,L_{\odot}$ or $<2.5 \times 10^{44}$ erg s^{-1}. The limit on the host continuum is $M_{1450} > -25.8$ mag.

Our observations of J1148+5251 have a depth similar to those of J1030+0524, yielding similar limits on the surface brightness (∼1×10^{-17} erg s^{-1} cm^{-2} arcsec^{-2} at 5σ significance, for a 1 arcsec^2 aperture). A bright spot is observed 1″ south of the quasar in the ON image (see Figure 2), but a careful inspection of the individual frames reveals that it is most likely a cosmic-ray residual. No other sources exceed the 5σ sensitivity limit for point sources (corresponding to Lyα luminosities of 2.6×10^{43} erg s^{-1}) within 1 arcmin^2 around the quasar.

5. DISCUSSION AND CONCLUSIONS

Our observations set limits on the extended emission of the UV continuum and of the Lyα emission in two quasar host galaxies at $z > 6$. The former are not very stringent (due to the narrow width of the filters adopted in our study). Using the UV continuum luminosity as a probe of star formation (Kennicutt 1998), we obtain a 2σ limit on the UV-based SFR of $<1200 M_{\odot}$ yr^{-1}, assuming a Salpeter initial mass function. These UV-based limits are in broad agreement with the FIR-based estimates of SFR ∼ 1700–3000 $M_{\odot}$ yr^{-1} reported for J1148+5251 (Maiolino et al. 2005; Walter et al. 2009) if a modest extinction correction ($A_{\rm UV} \approx 0.4$ mag) is applied.

On the other hand, the limits on the extended Lyα luminosity put tighter constraints on the physical properties of our targets. Two obvious sources of ionizing radiation are present in our targets, namely the accreting black holes and (at least for J1148+5251) the intense starburst seen at millimeter wavelengths. Both these processes are expected to power Lyα emission. If Lyα emission is powered by the quasar emission, we can estimate the expected Lyα emission from the host galaxies by modeling the interstellar medium (ISM) as cold gas clouds absorbing and re-emitting the light from the quasar. In this scenario, modulo geometrical factors of the order of unity, and assuming that the ISM clouds are optically thick to ionizing photons, the Lyα luminosity would be

$$L(\mathrm{Ly}\alpha) \approx 0.4\, f_{\rm c}\, L_{\rm ion.}, \quad (1)$$

where $f_{\rm c}$ is the covering factor of the clouds and $L_{\rm ion.}$ is the ionizing luminosity arising from the black hole accretion (J. F. Hennawi & J. X. Prochaska 2012, in preparation). Extrapolating the quasar SED observed in the rest-frame UV and optical wavelengths using the template by Elvis et al. (1994), we estimate that $L_{\rm ion.} \approx (3.3\text{–}5.4) \times 10^{46}$ erg s^{-1} for the two sources. Assuming $f_{\rm c} = 0.1$, we infer expected Lyα luminosities of ≈(1.3–2.2) × 10^{45} erg s^{-1}, i.e., one order of magnitude higher than the upper limits set by our observations (provided that the ISM clouds are distributed over a ∼ kpc scale or more, i.e., resolved in our observations).

If Lyα emission is associated with star formation, we can infer Lyα luminosities from the FIR-based estimates of the SFR (through the SFR–Hα relation reported in Kennicutt 1998), by assuming a standard case B recombination factor of 8.7 for the Lyα/Hα luminosity ratio:

$$\frac{L(\mathrm{Ly}\alpha)}{10^{43}\ \mathrm{erg\ s^{-1}}} = 0.11\ \frac{\mathrm{SFR}}{M_{\odot}}\ \mathrm{yr}^{-1}. \quad (2)$$

In the case of J1148+5251, with an SFR of 1700–3000 (Maiolino et al. 2005; Walter et al. 2009), this implies an expected Lyα luminosity of (1.9–3.3) × 10^{45} erg s^{-1}, i.e., one order of magnitude higher than the limit set by our observations.

This difference between expected Lyα luminosities and the observational constraints can be explained by invoking some mechanisms to suppress Lyα emission. Dust extinction is likely playing a role. A factor $\gtrsim$10 ($A_{\rm UV} > 2.5$ mag) of extinction is required to explain our limits. Such a high extinction value is not unexpected in FIR-bright sources, but is at odds with the relatively low extinction observed toward the central quasar: Gallerani et al. (2010) collected low-resolution spectroscopy of the rest-frame UV emission for a number of high-z quasars, including the two in our sample, and computed extinction values at 3000 Å (rest frame). They find no significant reddening for J1030+0524 and $A_{3000} = 0.82$ mag (i.e., $A_{\rm UV} \approx 1.3$ mag at the wavelengths probed in the present study) for J1148+5251. These relatively modest extinction values, compared with the limits set by our observations, suggest a different geometry for the highly opaque dust associated with the kpc-wide starburst and the optically thinner dust along the line of sight to the quasar (we note, however, that FIR-bright quasars tend to have faint Lyα nuclear emission as well; see, e.g., Wang et al. 2008a). Alternatively, resonance scattering may prevent Lyα emission from emerging out of the star-forming regions. While this effect alone is not sufficient to explain the lack of strong Lyα extended emission, it could mitigate the discrepancy if coupled with dust extinction. In this scenario, Lyα photons from the host repeatedly bounce among optically thick clouds through dusty regions, and become significantly extincted before escaping the host galaxy. Alternatively, Lyα emission may be dim due

to a deficit of neutral hydrogen around these bright quasars (see, e.g., Francis & Bland-Hawthorn 2004). This scenario, however, would be in contrast with the large reservoirs of cold gas observed at millimeter wavelengths.

It is interesting to compare our limits with the extended Lyα emission reported around another $z \sim 6$ quasar, J2329−0301 ($z = 6.417$). Goto et al. (2009) report a diffuse Lyα emission of 6.0×10^{-19} erg s^{-1} cm^{-2} Å^{-1} over an extended region ($R_e \approx 2''$) based on narrowband imaging with the 8.2 m Subaru telescope. This implies a diffuse Lyα luminosity of 3.6×10^{44} erg s^{-1}, comparable to the limits set by our observations.[10] More recently, the same group reported spectroscopic observations of the same source (Goto et al. 2012). The extended Lyα emission has an integrated flux of $(3.6 \pm 0.2) \times 10^{-17}$ erg s^{-1} cm^{-2}, i.e., 20 times fainter than the value reported in their imaging observations. Willott et al. (2011), using long-slit spectroscopy also, found evidence of extended Lyα emission around the same source. However, they report a *lower* limit on the Lyα flux of $>1.6 \times 10^{-16}$ erg s^{-1} cm^{-2} (the lower limit is due to slit losses and masking of the quasar-dominated area). These last values are comparable with the *upper* limits set by our observations. Following the same approach as in Willott et al. (2011), we re-analyzed the Keck HIRES spectra of J1030+0524 and J1148+5251 presented in Bolton et al. (2012). No Lyα emission is observed on scales exceeding the seeing radius, down to limits comparable with those set by our imaging study. If Lyα halos were present around the two targets examined in our work, they are less prominent than the one reported in J2329−0301.

We thank the anonymous referee for useful comments which improved the quality of the manuscript. We thank C. Leipski and E. Lusso for fruitful discussions on the quasar SEDs. Support for this work was provided by NASA through grant HST-GO-11640 from the Space Telescope Science Institute, which is operated by AURA, Inc., under NASA contract NAS5-26555. R.D. acknowledges funding from Germany's national research center for aeronautics and space (DLR, project FKZ 50 OR 1104). X.F. acknowledges support from NSF grant AST 08-06861 and a David and Lucile Packard Fellowship. M.A.S. acknowledges support of NSF grant AST-0707266.

[10] Goto et al. (2009) estimate a corresponding Lyα luminosity of 1.6×10^{42} erg s^{-1}, using $F(\mathrm{Ly}\alpha) = F_\lambda\ (\Delta v/c)\ \lambda_{\rm obs}\ f$, where $\Delta v = 300$ km s^{-1} is the line width, c is the speed of light, $\lambda_{\rm obs}$ is the observed wavelength of redshifted Lyα, and $f = 60\%$ is an Lyα to total (Lyα+cont) correction factor. However, we point out that in order to retrieve the correct estimate of the Lyα flux, one should use the filter width (≈1300 Å) instead of the expected line width (≈9 Å), making the true flux ∼100 times larger.

REFERENCES

Barrio, F. E., Jarvis, M. J., Rawlings, S., et al. 2008, MNRAS, 389, 792
Beelen, A., Cox, P., Benford, D. J., et al. 2006, ApJ, 642, 694
Bertoldi, F., Carilli, C. L., Cox, P., et al. 2003, A&A, 406, L55
Bolton, J. S., Becker, G. D., Raskutti, S., et al. 2012, MNRAS, 419, 2880
Carilli, C. L., Neri, R., Wang, R., et al. 2007, ApJ, 666, L9
Christensen, L., Jahnke, K., Wisotzki, L., & Sánchez, S. F. 2006, A&A, 459, 717
Dayal, P., Ferrara, A., Saro, A., et al. 2009, MNRAS, 400, 2000
Dekel, A., Birnboim, Y., Engel, G., et al. 2009, Nature, 457, 451
Di Matteo, T., Khandai, N., DeGraf, C., et al. 2012, ApJ, 745, L29
Dubois, Y., Pichon, C., Haehnelt, M., et al. 2012, MNRAS, 423, 3616
Elvis, M., Wilkes, B. J., McDowell, J. C., et al. 1994, ApJS, 95, 1
Fan, X., Narayanan, V. K., Lupton, R. H., et al. 2001, AJ, 122, 2833
Fan, X., Strauss, M. A., Schneider, D. P., et al. 2003, AJ, 125, 1649
Francis, P. J., & Bland-Hawthorn, J. 2004, MNRAS, 353, 301
Francis, P. J., & McDonnell, S. 2006, MNRAS, 370, 1372
Gallerani, S., Maiolino, R., Juarez, Y., et al. 2010, A&A, 523, 85
Goerdt, T., Dekel, A., Sternberg, A., et al. 2010, MNRAS, 407, 613
Goto, T., Utsumi, Y., Furusawa, H., Miyazaki, S., & Komiyama, Y. 2009, MNRAS, 400, 843
Goto, T., Utsumi, Y., Walsh, J. R., et al. 2012, MNRAS, 421, L77
Haiman, Z., & Rees, M. J. 2001, ApJ, 556, 87
Kennicutt, R. C. 1998, ARA&A, 36, 189
Kotilainen, J. K., Falomo, R., Decarli, R., et al. 2009, ApJ, 703, 1663
Leipski, C., Meisenheimer, K., Klaas, U., et al. 2010, A&A, 518, L34
Maiolino, R., Cox, P., Caselli, P., et al. 2005, A&A, 440, L51
Ouchi, M., Shimasaku, K., Furusawa, H., et al. 2010, ApJ, 723, 869
Peng, C. Y., Ho, L. C., Impey, C. D., & Rix, H.-W. 2002, AJ, 124, 266
Peng, C. Y., Ho, L. C., Impey, C. D., & Rix, H.-W. 2010, AJ, 139, 2097
Pentericci, L., Fan, X., Rix, H.-W., et al. 2002, AJ, 123, 2151
Priddey, R. S., Isaak, K. G., McMahon, R. G., Robson, E. I., & Pearson, C. P. 2003, MNRAS, 344, L74
Reuland, M., van Breugel, W., Röttgering, H., et al. 2003, ApJ, 592, 755
Riechers, D. A., Walter, F., Bertoldi, F., et al. 2009, ApJ, 703, 1338
Smith, D. J. B., Jarvis, M. J., Simpson, C., & Martínez-Sansigre, A. 2009, MNRAS, 393, 309
Volonteri, M., & Rees, M. J. 2006, ApJ, 650, 669
Walter, F., Bertoldi, F., Carilli, C., et al. 2003, Nature, 424, 406
Walter, F., Carilli, C., Bertoldi, F., et al. 2004, ApJ, 615, L17
Walter, F., Riechers, D., Cox, P., et al. 2009, Nature, 457, 699
Wang, R., Carilli, C. L., Beelen, A., et al. 2007, AJ, 134, 617
Wang, R., Carilli, C. L., Wagg, J., et al. 2008a, ApJ, 687, 848
Wang, R., Wagg, J., Carilli, C. L., et al. 2008b, AJ, 135, 1201
Wang, R., Wagg, J., Carilli, C. L., et al. 2011, AJ, 142, 101
Weidinger, M., Møller, P., Fynbo, J. P. U., & Thomsen, B. 2005, A&A, 436, 825
Willott, C. J., Chet, S., Bergeron, J., & Hutchings, J. B. 2011, AJ, 142, 186